



Study of Trailing-Edge Cooling Using Pressure Sensitive Paint Technique

Zifeng Yang* and Hui Hu†
Iowa State University, Ames, Iowa 50011

DOI: 10.2514/1.B34070

An experimental investigation was conducted to study the effects of blowing ratio and the existence of lands on the film cooling effectiveness of a turbine blade trailing-edge model. Instead of using a temperature-based technique, a mass transfer analogy was used to quantify the film cooling effectiveness. This was done through the measurement of the distribution of oxygen concentration over the surface of interest with airflow as the mainstream flow and nitrogen as the coolant stream. The pressure sensitive paint technique was used to map the distribution of the oxygen concentration on the surface of the cutback region of the trailing-edge model. The experimental study was conducted at five different blowing ratios between 0.4 and 1.6, both with and without moveable lands mounted on the trailing-edge model. The measurement results indicate clearly that the blowing ratio and the existence of the lands would affect the film cooling effectiveness of the trailing-edge design significantly. The detailed film cooling effectiveness maps were correlated with the characteristics of the flow structures revealed from the particle image velocimetry measurements to elucidate underlying physics and to explore and optimize design paradigms for a better protection of the critical portions of turbine blades from the extremely hot environment.

Nomenclature

C_{coolant}	=	oxygen concentration of cooling stream
C_{main}	=	oxygen concentration of mainstream
C_{mix}	=	oxygen concentration of the mainstream-coolant mixture
H	=	height of the coolant slot
I_b	=	intensity of the black image without light excitation
$I(P)_{\text{air}}$	=	intensity recorded with air as the coolant stream
$I(P)_{\text{mix}}$	=	intensity recorded with nitrogen as the coolant stream
$I(P)_{\text{ref}}$	=	intensity of the excitation light at the reference state (no flow)
L	=	length of the upper plate of the trailing-edge model
M	=	blowing ratio (i.e., mass flux ratio of the cooling stream and mainstream flow)
$(P_{\text{O}_2})_{\text{air}}$	=	partial pressure of oxygen with air as the coolant
$(P_{\text{O}_2})_{\text{mix}}$	=	partial pressure of oxygen with nitrogen as the coolant
P_{ref}	=	partial pressure of oxygen at reference state
Re_c	=	Reynolds number of the slot jets
T_{aw}	=	adiabatic wall temperature
T_c	=	temperature of the coolant stream
T_{∞}	=	temperature of the mainstream
t	=	lip thickness
U, V, W	=	X, Y, Z component of the flow velocity
U_c	=	velocity of the cooling stream
U_{∞}	=	velocity of the mainstream flow
η_{aw}	=	adiabatic cooling effectiveness

I. Introduction

THE requirement for higher turbine inlet temperatures in gas turbines and better thermodynamic efficiency has caused the

turbine blades to be critical components to protect. Without an appropriate cooling technique applied to turbine blades, the blades would not survive in the extremely hot environment. In various regions on turbine blades, several cooling techniques, such as internal convective cooling and film cooling on the blade exterior, are used widely in order to increase the lifetime of the blades. Film cooling is a state-of-the-art technique in protecting the key components in gas turbines. For the cooling of turbine blades, trailing edges are especially difficult to cool. In many reported damage cases, catastrophic failures commonly originate at the edges: trailing edges, tips, and roots of turbine blades. The thin trailing edges are very prone to thermal damage. In the present study, we are particularly concerned with the trailing-edge cutback regions of turbine blades, in which coolant slots are disrupted by stiffening lands. Usually, the trailing edges of turbine blades are cooled by slot jets of coolant, in which the pressure side of turbine blades is cut back a small length to form a characteristic step with spanwise slots to exhaust coolant streams.

A number of studies have been carried out in recent years to examine the trailing-edge cooling design of turbine blades. Taslim et al. [1] investigated the effects of different slot geometries on the film cooling effectiveness in the vicinity of the slot breakout region at various blowing ratios and density ratios. It was found that the ratio of lip thickness to slot height is a key parameter for the film cooling in the cutback region. Uzol et al. [2] and Uzol and Camci [3] investigated the aerodynamic loss characteristics of a turbine blade with trailing-edge coolant ejection. The effects of cutback length, spanwise rib spacing, freestream Reynolds number, and chordwise rib length on discharge coefficients were investigated. It was found that the discharge coefficients is almost independent of Reynolds number, therefore, the discharge coefficient experiments can be performed at relatively low Reynolds numbers. Martini et al. [4,5] conducted comprehensive studies on the discharge coefficients, film cooling effectiveness, and heat transfer coefficients on the trailing-edge cutback of gas turbine blades with various internal cooling designs. Holloway et al. [6,7] conducted both experimental and numerical studies on trailing-edge slots. It was found that trailing-edge cooling is not as effective as anticipated, i.e., hot gas reaches the surface more readily than expected. For instance, numerical simulations based on steady, Reynolds-averaged analysis approaches predicted notably better cooling effectiveness than the experimental measurements. The vortex shedding behavior from the lip of the slot exit was suggested to induce the fast decay of film cooling effectiveness for the cases with large t/H of the slot exit. More recently, numerical simulations of Medic and Durbin [8] and Joo and

Received 16 July 2010; revision received 12 November 2010; accepted for publication 11 January 2011. Copyright © 2011 by the American Institute of Aeronautics and Astronautics, Inc. All rights reserved. Copies of this paper may be made for personal or internal use, on condition that the copier pay the \$10.00 per-copy fee to the Copyright Clearance Center, Inc., 222 Rosewood Drive, Danvers, MA 01923; include the code 0748-4658/11 and \$10.00 in correspondence with the CCC.

*Postdoctoral Research Associate, Department of Aerospace Engineering; zyang@iastate.edu. Member AIAA.

†Associate Professor, Department of Aerospace Engineering; huhui@iastate.edu. Associate Fellow AIAA.

Durbin [9] revealed that three-dimensional unsteadiness, which occurs in cooling slot jets, is a primary cause of poor trailing-edge protection. This suggests a path to redesigning the coolant stream to alleviate the heat load. While Medic and Durbin [8] and Joo and Durbin [9] showed that the cooling jet stream contains unsteady, three-dimensional vortical components that have a significant effect on transporting heat and contaminants to the surface due to the coherent, three-dimensional vortex shedding from the upper lip of the breakout slot, the computational evidence has not been verified yet experimentally.

The film cooling effectiveness has been experimentally measured for many years. As more effective film cooling designs have been developed, techniques to determine the film cooling effectiveness have also progressed rapidly in recent years. Heat transfer experiments were traditionally used to quantify the film cooling effectiveness. Adiabatic film cooling effectiveness, η_{aw} , which was defined based on temperature measurements, is expressed as

$$\eta_{aw} = \frac{T_{\infty} - T_{aw}}{T_{\infty} - T_c} \quad (1)$$

where T_{∞} is the temperature of the main stream; T_{aw} is the adiabatic temperature of the surface of interest, and T_c is the temperature of the coolant stream.

In the earlier heat transfer experiments to investigate the film cooling of turbine blades, thermocouples were used to measure both fluid and surface temperatures. When used to measure surface temperatures, thermocouples can provide measurements only at limited discrete points [10]. Therefore, it is usually difficult to achieve temperature measurements (thereby, adiabatic film cooling effectiveness) with relatively high spatial and/or temporal resolutions based on the measurements with thermocouples. More recently, optical-based advanced thermometry techniques, which can achieve surface temperature distribution measurements with much higher spatial and temporal resolutions compared with the thermocouple-based measurements, have been used in both transient and steady heat transfer experiments for turbine blade cooling studies. The advanced thermometry techniques used for turbine blade cooling studies include liquid crystal thermometry [11], infrared thermometry [12]; laser induced fluorescence [13] and temperature sensitive paint [14] techniques. It should be noted, although useful information has been revealed from those temperature-based experiments, there always exists concerns and implications about the errors of the adiabatic temperature measurements on the surface of interest due to the effects of heat conduction through the test model in those heat transfer experiments.

Instead of conducting temperature measurements on the surface of interest, it becomes more and more popular to quantify the effectiveness of turbine blade cooling designs by conducting “cold” experiments with the pressure sensitive paint (PSP) technique [15,16]. The PSP technique used for film cooling effectiveness measurements is based on mass transfer analogy, which is free from heat conduction related measurement errors frequently encountered in the temperature-based experiments.

In PSP measurements, the surface of interest is coated with an oxygen sensitive paint layer. The paint layer consists of sensor molecules (luminophores) and binder material. Upon the excitation of photons at an appropriate wavelength [ultraviolet (UV) light source is usually used], the luminophores can emit photoluminescence light at a longer wavelength. In the presence of oxygen molecules, the ability of the luminophores to emit photoluminescence light is inhibited by a collision with oxygen molecules. The phenomenon is called oxygen quenching [15,16]. Higher concentration of oxygen would cause lower intensity of photoluminescence, and thus higher luminescent intensity indicates lower oxygen concentration.

To implement the PSP technique for film cooling effectiveness measurements on the surface of interest, airflow is usually used to represent the hot gas stream, while nitrogen is supplied to simulate the coolant stream. The mixing process between the hot gas flow and cold coolant stream in gas turbines is simulated by the dynamic

mixing between the airflow (i.e., oxygen concentration about 21%) and the nitrogen (i.e., oxygen free) over the surface of interest. By preventing the oxygen molecules from the mainstream flow (i.e., airflow) from reaching the surface of interest via nitrogen injection through the cooling holes, based on mass transfer analogy, the film cooling effectiveness distribution is determined in the term of oxygen concentration distribution over the surface of interest. With the concentrations of oxygen to replace the temperature in Eq. (1), the film cooling effectiveness can be expressed as

$$\eta = \frac{C_{main} - C_{mix}}{C_{main} - C_{coolant}} \quad (2)$$

When pure nitrogen is used as the coolant stream, $C_{coolant}$ will be zero. Since no heating is involved in the experiment, errors arising from heat conduction are eliminated completely, resulting in distinct and well-defined traces of the coolant streams.

In the present study, an experimental study was conducted to quantify the effects of blowing ratio of the coolant stream and the existence of lands on the effectiveness of film cooling over a typical turbine blade trailing-edge model. PSP technique was used to achieve detailed measurements of the film cooling effectiveness distributions on the surface of interest at different blowing ratios and with and without lands mounted on the trailing-edge model. The detailed film cooling effectiveness maps were correlated with the flow field measurements obtained by using a particle image velocimetry (PIV) system to elucidate underlying physics in order to explore new trailing-edge cooling strategies for a better protection of the critical portions of turbine blades.

II. Experimental Setup

A. Experimental Rig and Test Model

Figure 1 shows the schematic of the experimental setup used in the present study. The experiments were conducted in a low-speed, open-circuit wind tunnel that has a maximum velocity of 40 m/s located in the Aerospace Engineering Department of Iowa State University. The tunnel has an optically transparent test section of 8×5 in. (i.e., 200×125 mm) in cross section. The tunnel has a 10:1 contraction section upstream of the test section with honeycombs and screen structures installed ahead of the contraction section to provide uniform, low-turbulence incoming flow into the test section. The turbulence intensity in the center of the inlet of the test section was found to be about 1.0% of the incoming flow measured by using a hotwire manometer.

The test model used in the present study was designed to replicate only the trailing-edge portion of a typical turbine blade. As shown in

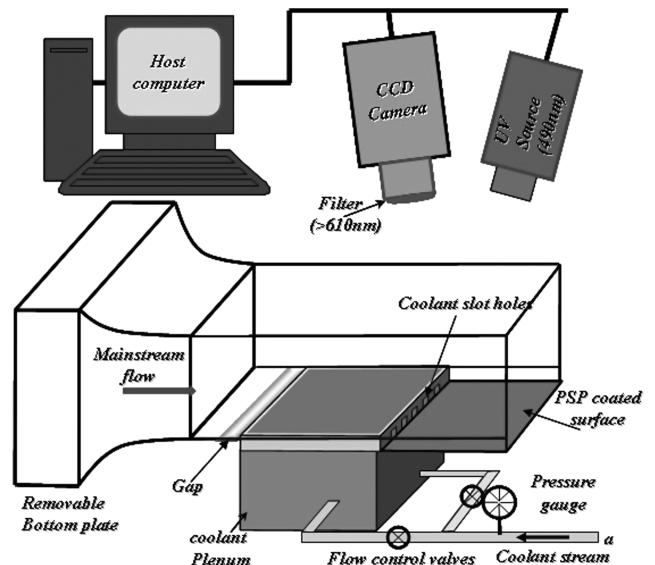
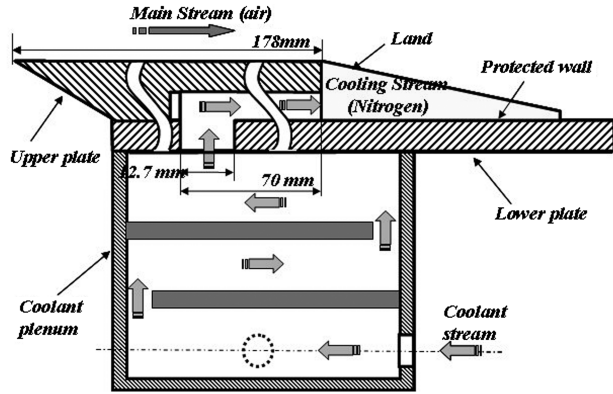
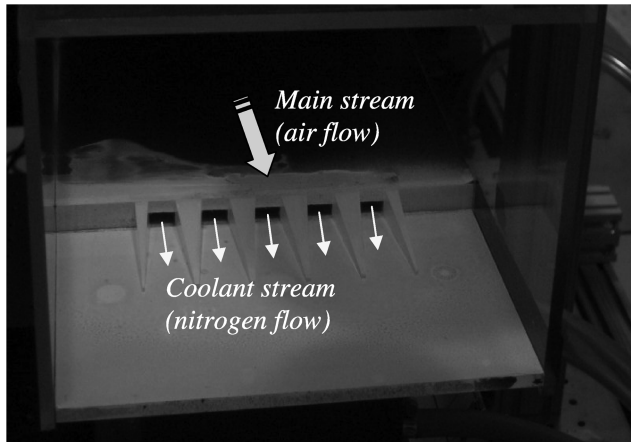


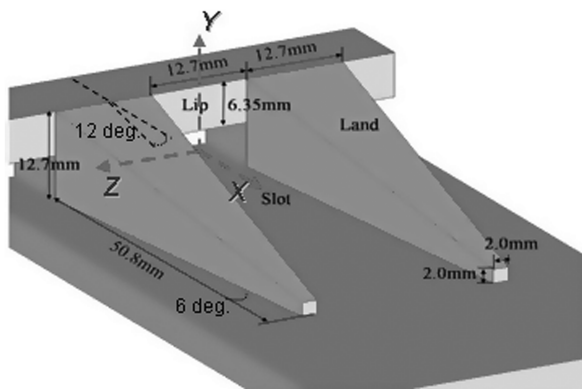
Fig. 1 Schematic of the experimental setup.



a) Side view of the trailing edge model



b) A perspective view of the trailing edge model



c) Zoom-in view of the central slot channel

Fig. 2 The trailing-edge model used in the present study.

Fig. 2, the trailing-edge model was simplified as a combination of two Plexiglas plates. The primary dimensions of the trailing-edge model were indicated in Fig. 2, which were chosen based on the geometry parameters listed in Taslim et al. [1]. In the present study, while air flow from the wind tunnel was supplied to simulate the hot gas flow, the coolant channel was fed by pure nitrogen to simulate the coolant stream to protect the cutback surface on the lower plate of the trailing-edge model. The mixing of the hot gas into the coolant flow at the trailing edge of a turbine blade was simulated by the mixing of mainstream airflow into the nitrogen stream over the surface of interest on the lower plate. As shown schematically in Fig. 2, a relatively large plenum (a cubic box with 152 mm in length, width and height), which is mounted underneath the lower plate, was designed to settle the coolant flow (i.e., nitrogen). Two partition plates were mounted inside the plenum in order to maintain a uniform flow condition for the coolant stream before exhausted through the

slot holes in the cutback region of the trailing-edge model. Five long slot channels were engraved into the bottom side of the upper plate to let the coolant stream exhausted from the coolant plenum onto the cutback region of the trailing-edge model as five slot wall jets. The turbulence intensity of the coolant stream at the exit of the slot holes was found to be about 7.0%, measured by using a hot wire anemometer. For the test cases with lands, six removable land pieces were mounted onto the lower plate of the trailing-edge model to form five flow channels along spanwise direction (i.e., Z-direction) in the cutback region. During the experiments, the upper plate of the test model was flush mounted on the bottom wall of the test section. A 25 mm streamwise gap was held between the bottom wall and the sharp leading edge of the trailing-edge model in order to remove the effects of the turbulent boundary layer from upstream.

In the present study, the main flow velocity at the inlet of the test section was set as $U_\infty = 16.2$ m/s. Based on the length of the upper plate ($L = 178$ mm) of the trailing-edge model, the corresponding Reynolds number is 1.9×10^5 . The experimental study was conducted at five different blowing ratios between 0.4 and 1.6, which is defined as the mass flux ratio of the cooling stream to mainstream flow (i.e., $M = \rho_c U_c / \rho_\infty U_\infty$). The small density difference between the coolant stream (nitrogen) and mainstream airflow is neglected in the present study. The corresponding Reynolds number of the coolant stream, Re_c , is in the range of 2800 to 10,500 (based on the height of the slot, H). The flow parameters were found to be in the same range as those used in Martini and Schulz [4] and Choi et al. [17].

During the experiments, an air conditioning system was used to maintain the temperature of the mainstream airflow at 22°C. The coolant flow, which was supplied from a purified nitrogen gas cylinder or a high-pressure air tank depending on the requirement of the measurement, passed through flow control valves to enter the coolant plenum. The lower plate surface of the test model was sprayed with Binary UniCoat PSP supplied by Innovative Scientific Solutions, Inc.. A constant UV light with a wavelength of 400 ± 5 nm was used as the excitation source for the PSP measurements. A charge-coupled device (CCD) camera (PCO 1600, Cooke Corp.) with a 610 nm filter was used to records the intensity of the photoluminescence light emitted by the excited PSP molecules. Since the Binary UniCoat paint used in the present study is slightly temperature sensitive, a thermometer was used to measure the temperature variations on the surface of interest in order to compensate the effects of the temperature variations on the film cooling effectiveness measurement results.

B. Film Cooling Effectiveness Measurement Theory and Data Analysis

As previously described, since the photoluminescence intensity of the excited PSP molecules is a function of the concentration of oxygen molecules (i.e., oxygen partial pressure), the quantitative information about the distributions of the oxygen concentration over the surface of interest can be obtained from an intensity ratio along with a PSP calibration curve. The oxygen concentration information can be directly converted into static pressure distributions for the case with air flow as the coolant stream. Intensity ratios for air and air-nitrogen mixture can be expressed as Eqs. (3) and (4), respectively:

$$\frac{I(P)_{\text{ref}} - I_b}{I(P)_{\text{air}} - I_b} = f((P_{\text{O}_2})_{\text{air}}; P_{\text{ref}}) \quad \text{or} \quad f(P; P_{\text{ref}}) \quad (3)$$

$$\frac{I(P)_{\text{ref}} - I_b}{I(P)_{\text{mix}} - I_b} = f((P_{\text{O}_2})_{\text{mix}}; P_{\text{ref}}) \quad (4)$$

Where the reference intensity (with illumination, no flow, surrounding pressure uniform at 1.0 atm) is required in order to determine the intensity ratio, and black image (no illumination and no flow) intensity is used to remove the effects of camera noise. With a PSP calibration curve, the partial pressure of oxygen (i.e., oxygen concentration) on the surface of interest with both air and nitrogen as the coolant stream can be calculated. Then, the film

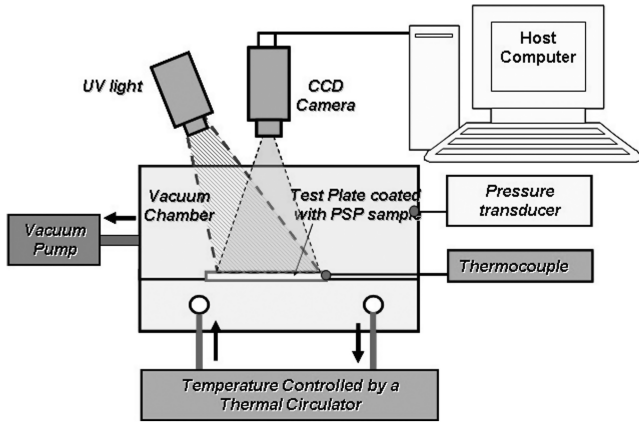


Fig. 3 Schematic layout of the calibration setup.

cooling effectiveness can be expressed as the ratio of the oxygen concentrations measured by PSP technique with the following equation:

$$\eta_{aw} = \frac{C_\infty - C_{mix}}{C_\infty} = \frac{(P_{O_2})_{air} - (P_{O_2})_{mix}}{(P_{O_2})_{air}} \quad (5)$$

Figure 3 depicts a schematic of the system setup used in the present study to determine the PSP calibration curve. To perform the PSP calibration, a test plate was sprayed with Binary UniCoat PSP. Air was removed from the test chamber by a vacuum pump, and the photoluminescence intensity of the excited PSP molecules was calibrated with the pressure in the vacuum chamber varied from 23.0–101.3 kPa. At each measurement point, the PSP molecules were excited by using a UV light at the wavelength of 400 ± 5 nm. The CCD camera with a 610 nm filter was used to records the images. A water circulation system was used to adjust the temperature of the test plate, which was monitored by using a thermocouple. Since the ambient temperature for the trailing-edge cooling experiments was 22°C , the temperature of the test plate was set at the same temperature during the calibration. The PSP calibration curve, which was based on the averaged intensity ratio and the averaged pressure data measured by using a pressure transducer (DSA 3217 16PX 1.0PSID, Scanivalve, Corp.), is shown in Fig. 4, where the measurement data were fitted to a polynomial curve. Further information about the experimental setup and PSP calibration procedure is available in [18].

C. Discussions About Measurement Uncertainties

With the perspective angle of the camera used for the PSP measurements, the complicated three-dimensional structures of the trailing-edge model might induce some measurement errors in the

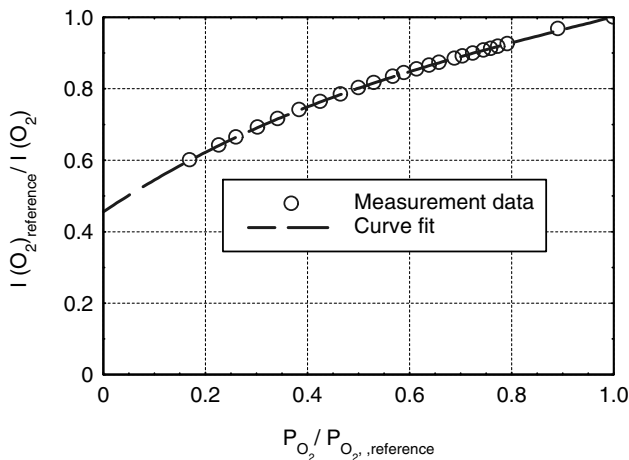


Fig. 4 PSP calibration curve.

two-dimensional views. The vertical surfaces of the lips of the slot exits and lands would be revealed as thin regions around the coolant slots in the cutback region. However, for the measurements given in the present study, it is assumed that all the measurement data only represent the information from the top surfaces of the lips and the lands in the cutback region. This would induce measurement errors in those regions. The width of the regions was estimated to be about 2 mm (about $1/3$ of H). Since the Binary UniCoat PSP paint used in present study is temperature sensitive to some extent, even though the temperature difference between the mainstream air flow and the coolant nitrogen flow was found to be only about 1°C at the low blowing ratio of $M = 0.4$, and about $2 \sim 3^\circ\text{C}$ at higher blowing ratios, the temperature difference will result in measurement uncertainties in the PSP measurements. Following the work of Kline and McClintock [19], the measurement uncertainty of the present study was estimated, which was found to be about $4 \sim 5\%$ for the oxygen partial pressure distribution, and about 9% for the film cooling effectiveness measurement results.

III. Results and Discussions

A. Effects of Blowing Ratios on Film Cooling Effectiveness for Cases Without Lands

As previously described, the coolant stream would be exhausted from the five slot holes as five slot jets aligned along spanwise direction in the cutback region of the test model. The PSP measurement results revealed a very similar pattern at the downstream of the exits of the five coolant holes in the term of film cooling effectiveness distributions. To reveal the characteristics of the trailing-edge cooling more clearly, only the film cooling effectiveness distribution at the downstream of the exit of the central slot hole was shown in the present study. Figure 5 shows the map of the film cooling effectiveness in the cutback region at different blowing ratios without the lands mounted onto the trailing-edge model. The film cooling effectiveness distributions are indications of the intensive mixing between coolant streams and mainstream flow at different blowing ratios. At low blowing ratio of $M = 0.4$, neighboring coolant jet streams were found to coalesce in the near field, resulting in a large region with uniform and high film cooling effectiveness (i.e., $\eta_{aw} > 0.90$) near to the exit of the coolant slot hole. The film cooling effectiveness was found to decay rapidly downstream of $X/H > 5.0$, and reaches to $\eta_{aw} \approx 0.45$ at the downstream location of $X/H \approx 8.0$. As the blowing ratio increases, the higher momentum of the coolant stream was found to restrain the coalescence of the neighboring coolant jet flows. Corresponding to the core region of the coolant jet flows, the region with high film cooling effectiveness at the downstream of the exit of the slot hole was found to become longer and longer with the increasing blowing ratio. It indicates that, as the blowing ratio increases, the coolant stream would tend to cover more area along the streamwise direction at the downstream of the slot hole. The mainstream flow was found to be more ready to mix onto the surface of the cutback region in the regions between the neighboring coolant jet streams, resulting in relatively low film cooling effectiveness on the surfaces of the “gap” regions. The feature becomes more and more apparent as the blowing ratio increases. The measurement results suggest that it is easier for the coolant stream to spread out and create more uniform coverage along spanwise direction at relatively low blowing ratios. As the blowing ratio increases, the higher momentum of the coolant stream would restrict the spanwise spreading of the coolant stream, thus, it would become more difficult for the coolant stream to cover the gap regions between the neighboring coolant jet flows. The measurement results suggest that, optimizing the blowing ratio involves finding a balance between the more uniform spanwise coverage and the longer streamwise coverage at the downstream of exit of the slot hole. It should also be noted that, the maximum values of the measured film cooling effectiveness were found to be around 1.0 for all test cases shown in Fig. 5, which is difficult to be obtained by the measurements of those heat transfer experiments due to the effects of heat conduction.

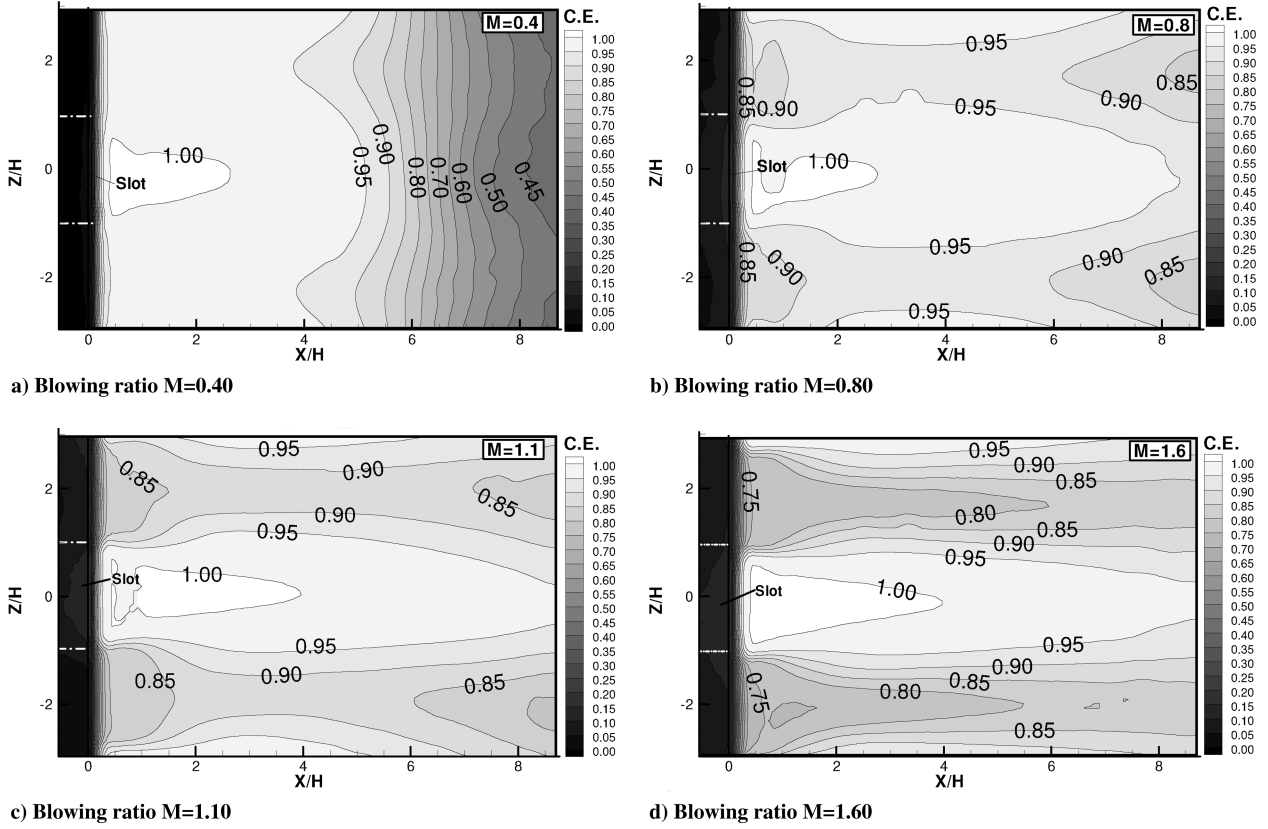


Fig. 5 Film cooling effectiveness distributions at different blowing ratios without lands.

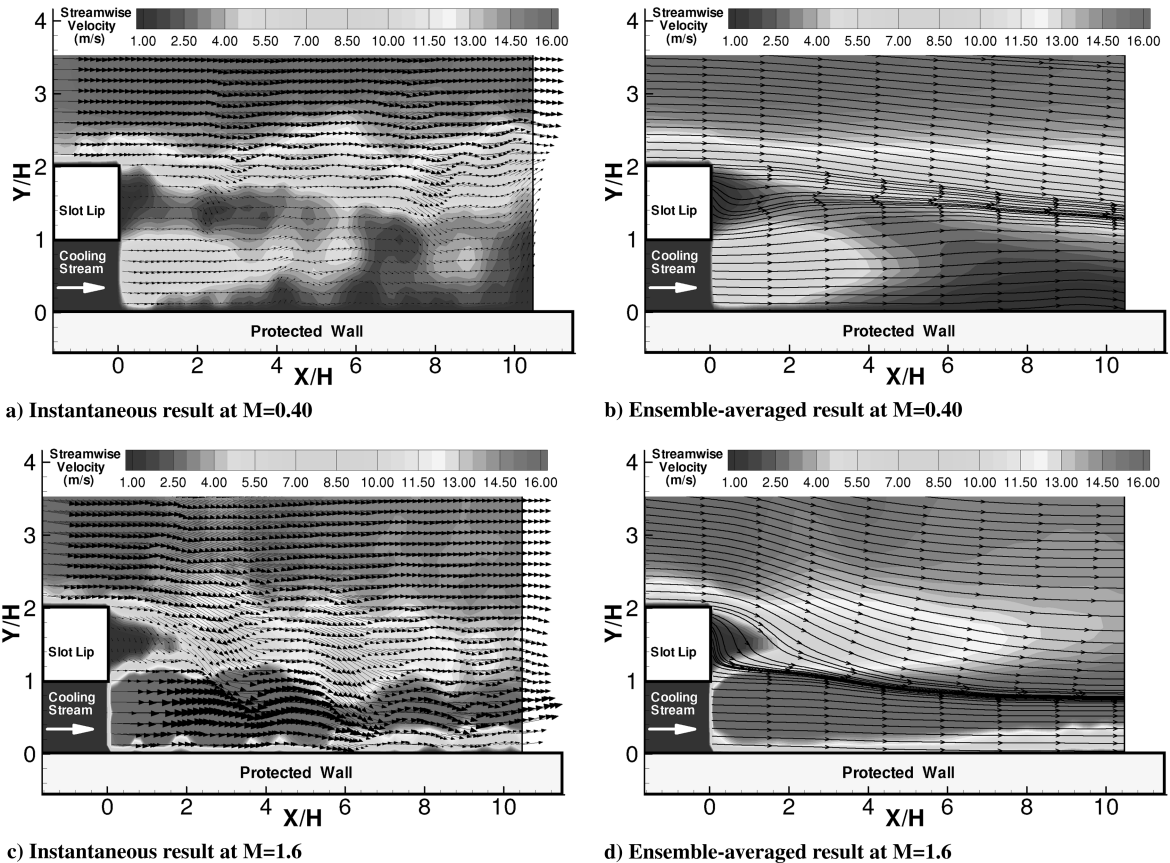
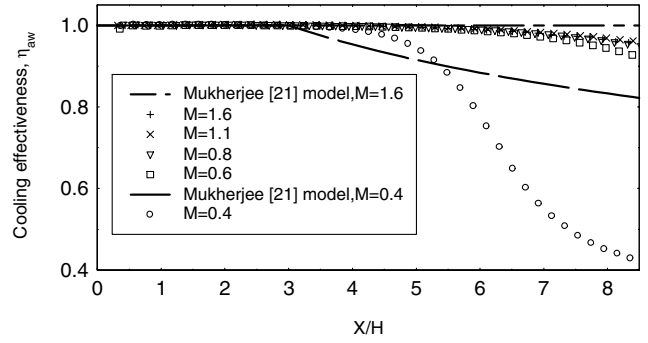


Fig. 6 PIV measurement results along the middle plane of the coolant jet flow.

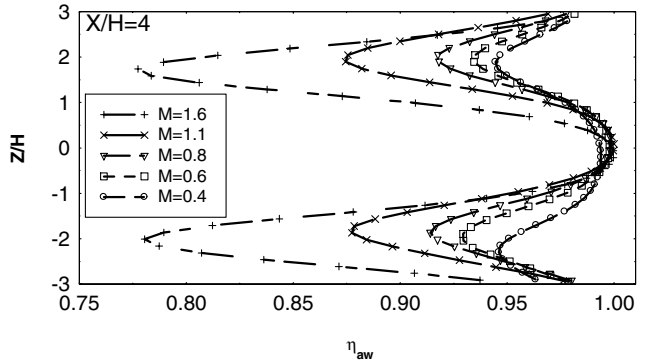
To gain more insight into the underlying physics pertinent to the trailing-edge cooling, Yang [18] conducted detailed PIV measurements to characterize the dynamic mixing between the mainstream flow and coolant stream over the trailing-edge model used in the present study. While further detailed information and discussions about the PIV measurements are available at Yang [18], some typical PIV measurement results were shown in the present study to facilitate the understanding of the characteristics of trailing-edge cooling revealed from the PSP measurements. Figure 6 shows the typical PIV measurements along the middle plane of the coolant jet flows at two typical blowing ratios, i.e., $M = 0.4$ and $M = 1.6$. It can be seen clearly that, for the case at low blowing ratio of $M = 0.4$, the mainstream flow has little effects on the evolution of the coolant stream in the near region close to the exit of the slot hole. After the coolant stream was exhausted from the exit of the slot hole, it could cover the cutback surface nicely in the near region, which results in almost perfect film cooling effectiveness in the near field downstream the exit of the slot hole as revealed in the PSP measurements. It was also revealed that, vortex structures shedding from the thick lip of the slot hole would interact with the coolant stream and mainstream flow, resulting in an intensive mixing between the mainstream flow and the coolant stream at further downstream of the slot exit. As a result, the film cooling effectiveness further downstream of the slot exit (i.e., $X/H > 5.0$) was found to decrease rapidly, as revealed from the PSP measurements shown in Fig. 5. Similar phenomena were also observed by Martini and Schulz [4], Telisinghe et al. [20] and Choi et al. [17].

For the case at higher blowing ratio of $M = 1.6$, the coolant stream would have much higher momentum to dispel the mainstream flow away from the surface of interest at the downstream of the slot exit, which results in higher film cooling effectiveness over the surface of interest. Because the intensive mixing between the coolant stream and the mainstream flow, the high-speed region of the coolant stream was found to become thinner and thinner with the increasing downstream distance. As shown clearly in the PIV measurement results shown in Fig. 6, since the coolant stream was still able to cover the surface of interest nicely, the mainstream flow was found to be driven out from the near wall region up to $X/H > 10$ downstream of the slot exit. Therefore, there is no apparent decrease of the film cooling effectiveness along the centerline of the coolant jet flow, which was confirmed quantitatively by the PSP measurement results given in Fig. 5.

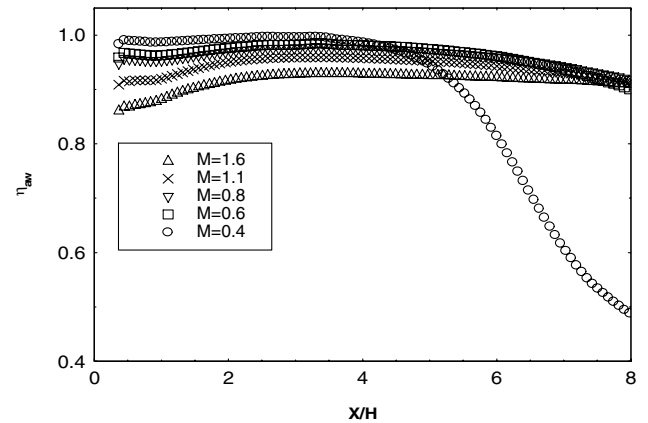
To reveal the effects of blowing ratio on the film cooling effectiveness over the surface of the cutback region more clearly and quantitatively, the profiles of the film cooling effectiveness along the centerline (i.e., $Z/H = 0$) of the coolant jet flow as a function of downstream distance at various blowing ratios were plot in the same graph, which are shown in Fig. 7a. It can be seen clearly that, at the low blowing ratio of $M = 0.4$, the film cooling effectiveness was found to decrease drastically in the downstream region of $X/H > 5.0$. All the other profiles were found to follow a similar trend with the film cooling effectiveness decreasing slightly with the increasing downstream distance, which is almost independent of the blowing ratio. Based on the theoretical model of Mukherjee [21], the predictions of the film cooling effectiveness for the tangential slot film cooling over a flat plate at blowing ratio of $M = 0.4$ and $M = 1.6$ were also given in the graph for comparison. It can be seen clearly that a generally good agreement between the theoretical prediction and the experimental measurements was obtained for the case with high blowing ratio of $M = 1.6$, with the theoretical model slightly overpredicted the experimental measurements at the downstream of $X/H > 6.0$. However, for the case with low blowing ratio of $M = 0.4$, a significant difference was found between the theoretical prediction and the measurement results. This may be explained by the fact that, Mukherjee's theoretical model was developed with the assumption of a two-dimensional slot jet flow, while the coolant jet streams of the present study are discrete jet flows. As shown clearly in Fig. 5, the spanwise spreading of the coolant stream at low blowing ratios was found to be much more pronounced compared with that at high blowing ratios, therefore, the effects of the three-dimensionality of the coolant jet flows was found to become more severe at low



a) Along the centerline of the coolant jet at $Z/H=0.0$



b) At the downstream location of $X/H=4.0$



c) Spanwise averaged film cooling effectiveness

Fig. 7 Film cooling effectiveness profiles for the cases without lands.

blowing ratios. Furthermore, the lip thickness was assumed to be zero in the Mukherjee's theoretical model, while the ratio of lip thickness to slot height was 1.0 for the present study. As described clearly in Mukherjee [21], the zero lip thickness assumption would result in overestimation of the film cooling effectiveness. As a result, for the case with a low blowing ratio of $M = 0.4$, the measured film cooling effectiveness was found to be much lower compared with the theoretical prediction based on the Mukherjee's model. Similar observations were also reported by Choi et al. [17]. It is noted that, Mukherjee [21] also suggested that the overestimation in film cooling effectiveness due to the nonzero lip thickness assumption would become less significant with the increasing blowing ratio, which was confirmed by the present study as less discrepancies between the theoretical prediction and the measurement results were found at the high blowing ratio of $M = 1.6$.

As shown in Fig. 7b, the comparison of the film cooling effectiveness profiles along spanwise direction at the downstream location of $X/H = 4$ reveals an apparent difference at different blowing ratios. All the profiles were found to reach the peak value of

$\eta_{aw} \approx 1.0$ at the position of $Z/H = 0$ (i.e., along centerline of the coolant jet flow), which indicates a perfect film cooling effectiveness in the region. The film cooling effectiveness was found to decrease rapidly with the increasing distance away from the centerline of the coolant jet flow along spanwise direction, and reach the lowest values at the location of $|Z|/H \approx 2.0$, which is at the centerline of the region between the neighboring coolant jet flows, i.e., gap region in short. The film cooling effectiveness in the gap region was found to decrease drastically as the blowing ratio increases. The observation can be explained in correlation with the less spanwise spreading of the coolant stream at higher blowing ratios in the gap region, as previously described.

Figure 7c shows the spanwise-averaged film cooling effectiveness (the averaged area covers the region between $Z/H = -2.0$ and $Z/H = 2.0$) as a function of the downstream distance at different blowing ratios. It can be seen clearly that, the spanwise-averaged film cooling effectiveness would decrease with the increasing blowing ratio except for the case with the lowest blowing ratio of $M = 0.4$ at the downstream region of $X/H > 4.0$. Such observation is believed to be closely related to the less spanwise spreading of the coolant streams at higher blowing ratios. It is noted that the observation is found to disagree with the findings of Martini and Schulz [4], who suggested that a higher film cooling effectiveness will be reached at the higher blowing ratio. The disagreement is believed to be mainly caused by the different design of trailing-edge models used by the two studies. It should also be noted that the coolant-to-mainstream density ratio was quite different for the present study compared with those of Martini and Schulz [4]. While the coolant-to-mainstream density ratio is about 1.0 for the present cold study (i.e., no temperature differences between the coolant stream and mainstream flow), the density ratio of the “hot” study of Martini and Schulz [4] was found to be about 1.6 with significant temperature differences between the coolant and mainstream flows. A systematic study is planned to investigate the effects of coolant-to-mainstream density ratio on the film cooling effectiveness in the near future.

B. Effects of Blowing Ratios on Film Cooling Effectiveness for Cases with Lands

PSP measurements were also conducted for the cases with six land pieces mounted onto the lower plate of the trailing-edge model. With the six land pieces mounted onto the test model, the coolant stream exhausted from the five slot exits were separated into five channel flows along the spanwise direction. As previously described, since the measurement results in the five slot channel were found to be almost identical, only the distribution of the film cooling effectiveness over the central unit, which includes the bottom surface of the central slot channel and tops surfaces of the neighboring lands, are shown in the present study. While the experimental study was carried out at five different blow ratios between 0.4 and 1.6, Fig. 8 shows the film cooling effectiveness distributions at four typical blowing ratios. It can be clearly seen that, the regions with relatively high film cooling effectiveness were found to concentrate in the center of the slot channel, as expected. The magnitude of the film cooling effectiveness in the regions was found to be about 1.0, which indicates that the coolant stream could protect the surface almost perfectly, and the mainstream flow would be dispelled away from the surface in those regions. At the blowing ratio of $M = 0.4$, the film cooling effectiveness along the centerline of the slot channel was found to drop to about 0.9 at the downstream of $X/H > 4.5$ for the present study. Choi et al. [17] reported that the film cooling effectiveness would decrease slightly slower compared with the findings of the present study, which would decrease to about 0.9 at the downstream of $X/H > 6.0$. The discrepancy may be attributed to the different Reynolds numbers of the coolant jet flows (i.e., $Re_c = 2800$ for the present study and $Re_c = 5000$ for Choi et al. [17]) as well as the different design parameters of the trailing-edge models used in the two studies.

It can also be seen clearly that the top surfaces of the lands surrounding the slot channel were found to have relatively low film cooling effectiveness. Compared with those shown in Fig. 5, the values of the film cooling effectiveness on the top surfaces of the lands were found to be much smaller compared with those in the “gap

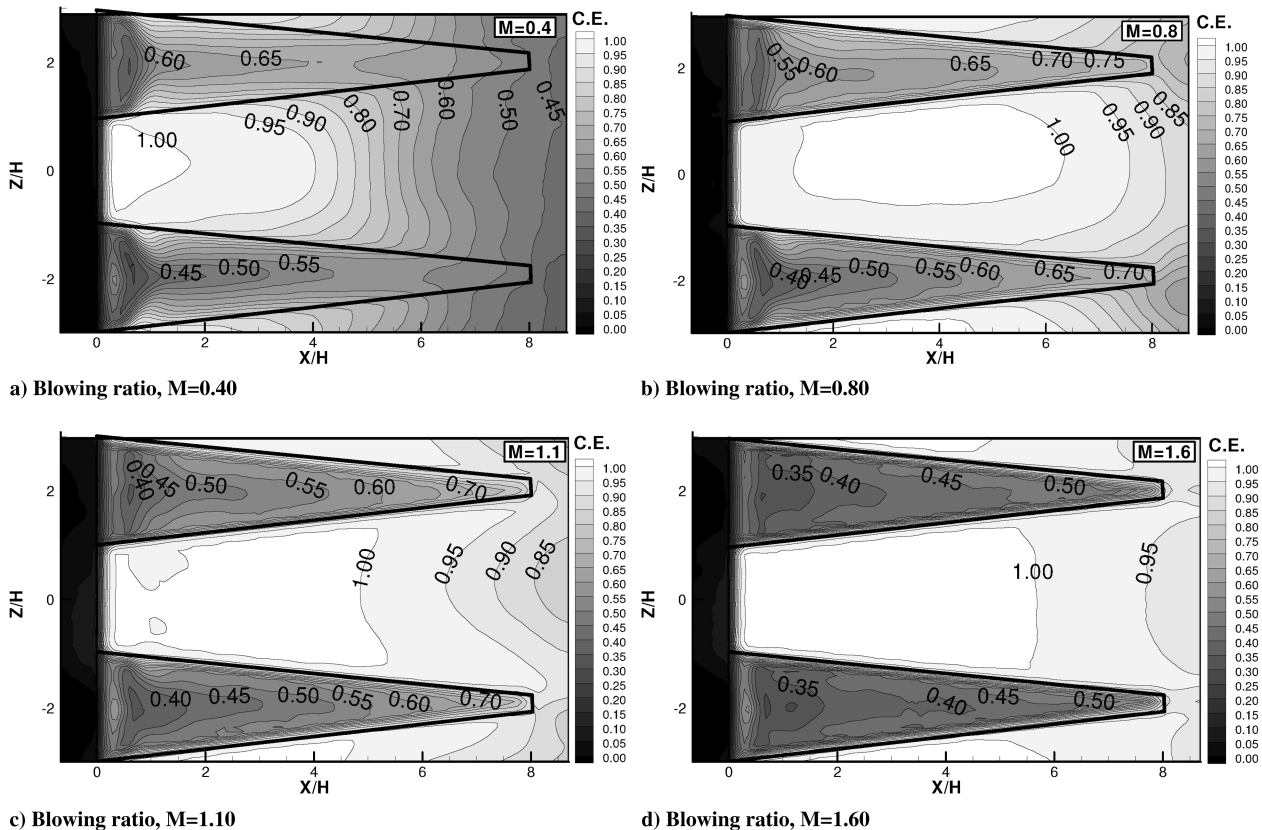


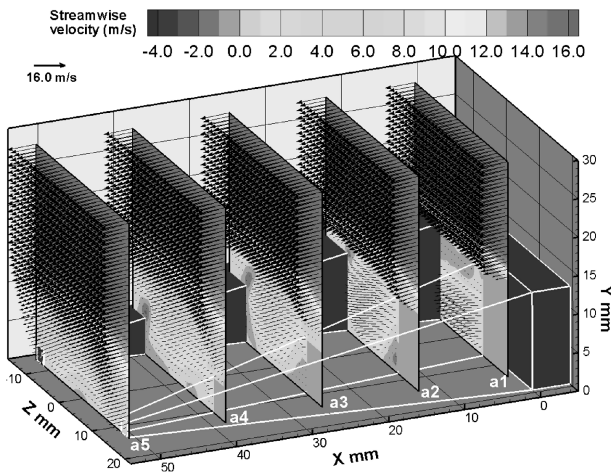
Fig. 8 Film cooling effectiveness at different blowing ratios for the cases with lands mounted onto the test model.

regions” for the cases without the lands mounted onto the surface of the trailing-edge model. This can be explained by the facts that the land pieces would serve as the barriers to guide the coolant stream flowing smoothly inside the slot channel. It will be much difficult for the coolant stream to climb up to cover the top surfaces of lands compared with the spanwise spreading of the coolant stream over the surface of the lower plate of the trailing-edge model to protect the gap regions.

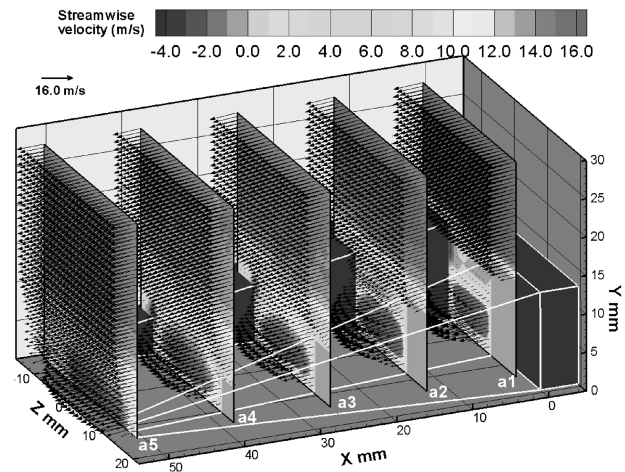
As the blowing ratio increases, the momentum of the coolant stream would become higher and higher, which would have stronger power to blow the mainstream flow away from the surface of interest. As a result, the regions with almost perfect film cooling effectiveness inside the slot channel were found to become bigger and bigger. It is also worthy of note that, while the contour lines of the film cooling effectiveness near the center of the slot channel was found to be bulged outward to extend further downstream for the cases with the blowing ratio smaller than 1.0 (i.e., $M < 1.0$), the contour lines were found to be bulged inward to face upstream for the cases with the blowing ratio greater than 1.0 (i.e., $M > 1.0$). Similar features were also revealed in the numerical simulation results of Joo and Durbin [9]. The observation is believed to be closely related to the characteristics of the flow structures generated in the cutback region of the trailing-edge model.

As previously described, with the same trailing-edge model used in the present study, Yang [18] conducted detailed flow field measurements to quantify the dynamic mixing process between the coolant stream and mainstream flow by using a high-resolution stereoscopic PIV system. The time sequence of the instantaneous PIV measurements revealed clearly that the mixing process between the coolant stream and mainstream flow in the cutback region would be changed significantly due to the existence of the lands. While further details about the stereoscopic PIV measurements at different

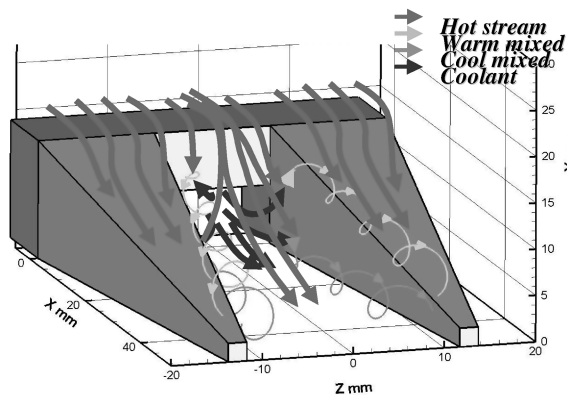
blowing ratios can be found at Yang [18], Figs. 9a and 9b show the ensemble-averaged results of the stereoscopic PIV measurements at the blowing ratio $M = 0.4$ and $M = 1.6$, respectively. Based on the PIV measurements as those shown in Figs. 9a and 9b, the schematics of the streamlines and vortex structures in the cutback region were derived, which were shown in Figs. 9c and 9d. It can be seen clearly that, a series of streamwise vortices would be generated at the corners of the coolant slot channel, which are closely related to the mixing process of the coolant stream with the mainstream flow in the cutback region. For the cases with the blowing ratio smaller than 1.0 (i.e., $M < 1.0$), the coolant stream will be entrained by the high-momentum mainstream flow. When viewing from upstream along the streamlines of the coolant stream, the streamwise vortices at the left corners of the slot channel were found to be counterclockwise, while the vortices at the right corners of the slot channel were clockwise. As a result, the streamwise vortices would promote the coolant stream climbing up around the edges of the lands to cover the top surfaces of the lands, which contributed to the relatively good film cooling effectiveness on the top surfaces of the lands at relatively low blowing ratios. Conversely, as the blowing ratio becoming great than 1.0, the mainstream flow would be entrained by the high-momentum coolant stream. After exhausted from the coolant slot exit, the high-momentum coolant stream would more readily flow along the slot channel and provide a better protection over the bottom surface of the slot channel, which results in almost perfect film cooling effectiveness on the surface inside the slot channel as revealed from the PSP measurements. The streamwise vortices at the corners of the slot channel were found to reverse their direction with the clockwise vortices at the left corners and counterclockwise vortices at the right corners of the slot channel as the blowing ratio becoming greater than 1.0. The streamwise vortices would limit the climbing up of the coolant stream to cover the top surfaces of the



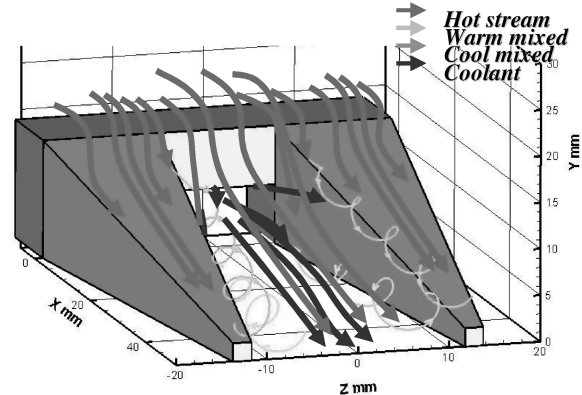
a) Stereo PIV measurement result at $M=0.40$



b) Stereo PIV measurement result at $M=1.60$



c) Schematic of the flow structures at $M < 1.0$



d) Schematic of the flow structures at $M > 1.0$

Fig. 9 Flow structures near the cutback region of the trailing-edge model.

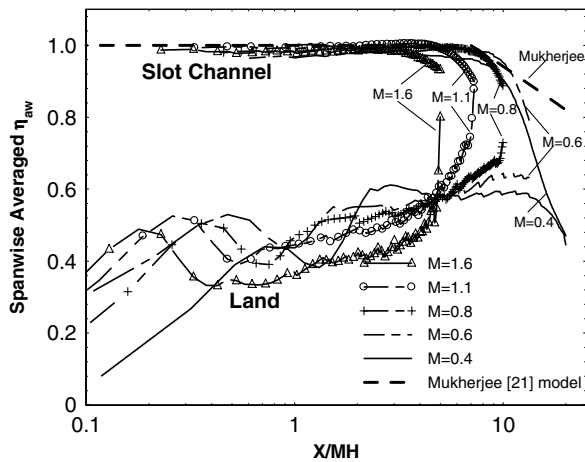


Fig. 10 The profiles of the spanwise-averaged film cooling effectiveness.

lands. It would result in the relative low film cooling effectiveness on the top surfaces of the lands, as confirmed from the PSP measurement results shown in Fig. 8. Since the coolant stream with higher momentum would more readily flow inside the slot channel as the blowing ratio increases, the film cooling effectiveness on the tops of the lands was found to become lower and lower. Similar phenomena were also revealed by the numerical simulations of Chen et al. [22].

Figure 10 shows the profiles of the spanwise-averaged film cooling effectiveness on the bottom surface of the slot channel and the top surfaces of the lands at five different blowing ratios. The measurement results were also compared with the theoretical prediction of Mukherjee [21] for the tangential slot film cooling on a flat plate with no pressure gradient and zero lip thickness. As shown in the figure, a reasonably good agreement between the measurement results and the theoretical prediction of Mukherjee [21] was obtained for the spanwise-averaged cooling effectiveness on the bottom surface of the slot channel. As previously described, the spanwise spreading of the coolant stream was suggested to be the primary reason to cause the disagreement between the measured cooling effectiveness and the theoretic prediction of Mukherjee [21] for the cases without lands mounted on the trailing-edge model. With the lands mounted on the trailing-edge model, the lands would guide the coolant stream flowing smoothly along the slot channel to protect the surface of interest in the cutback region. Since the spanwise spreading of the coolant stream was restricted by the existence of the lands, the theoretical model of Mukherjee [21] would make a better prediction of the film cooling effectiveness on the bottom surface of the slot channel, as expected.

As previously described, since the coolant stream needs to climb up the lands in order to cover the top surfaces of the lands, the spanwise-averaged cooling effectiveness on the top surfaces of the lands was found to be quite low in the region near the exit of the coolant slot. Corresponding to the decreasing height of the lands along the streamwise direction, the spanwise-averaged cooling effectiveness on the top surfaces of the lands was found to increase gradually as the downstream distance increases. The profiles of the film cooling effectiveness on the bottom surface of the slot channel was found to converge with those of the top surfaces of the lands further downstream near the ends of the lands.

Figure 11 shows the comparison of the overall-averaged cooling effectiveness on the surface of the cutback region as a function of the blowing ratio for the two different turbine trailing-edge designs. The overall-averaged film cooling effectiveness data were obtained by spatially averaging the all the measurement data in the region between $Z/H = -2$ and $Z/H = 2$ in spanwise direction and $X/H = 0$ and $X/H = 8.0$ in streamwise direction for the cases with and without the lands mounted on the trailing-edge model. The profiles of the overall-averaged film cooling effectiveness were found to reach their peak values at the blowing ratio of $M = 0.6 \sim 0.8$, and then decrease with the increasing blowing ratio, which does not agree with

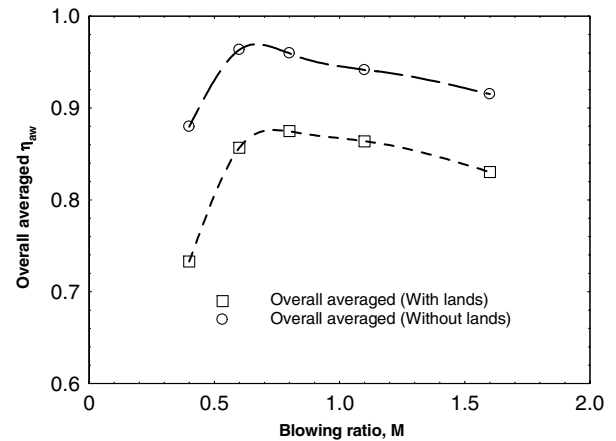


Fig. 11 The overall-averaged film cooling effectiveness vs the blowing ratio.

the monotonous decreasing trend reported by Choi et al. [17]. This may be attributed to the different configurations of the trailing-edge designs used by the two studies, especially for the inclining angle of the coolant slot to the mainstream flows. It can also be seen that, the case without lands would have higher overall-averaged film cooling effectiveness in general. The lower overall-averaged film cooling effectiveness for the case with lands is mainly because of the worse film cooling effectiveness on the top surfaces of the lands. It should be noted that, it does not necessarily mean that the trailing-edge design without lands would be better than the design with lands, since the overall performance of a turbine trailing-edge design would also include the considerations of heat transfer through heat conduction, structural strength and system integrity. The trailing-edge design with lands will definitely perform better in the terms of heat transfer through conduction, structural strength and system integrity, compared with the design without lands. Further investigations are needed to explore/optimize design paradigms for better protection of the critical portions of turbine blades from the harsh gas path conditions.

IV. Conclusions

An experimental study was conducted to investigate the effects of blowing ratio and the existence of lands on the effectiveness of film cooling over the cutback surface of a turbine trailing-edge model. PSP technique was used to map the distributions of the film cooling effectiveness on the surface of interest based on mass transfer analogy. The measurement results revealed clearly that, for the case without lands mounted on the trailing-edge model, higher blowing ratio would result in better film cooling effectiveness on the surface of interest along the streamwise direction, but worse film cooling effectiveness along the spanwise direction. Optimization of the blowing ratio involves balancing between the spanwise coverage and the streamwise coverage of the coolant stream over the surface of interest. With the lands mounted onto the trailing-edge model, the lands would act as the side walls of the slot channels at the downstream of the coolant slot exits. As the coolant stream exhausted from the slot exits, the lands would guide the coolant stream flowing smoothly inside the slot channels to protect the bottom surfaces of the slot channels, which leads to an almost perfect cooling effectiveness on the bottom surface of the slot channel. However, the spanwise spreading of the coolant stream would be restricted by the existence of the lands, which results in relatively poor film cooling effectiveness on the top surfaces of the lands. The best overall cooling effectiveness was found to be achieved at the blowing ratio of $M = 0.6 \sim 0.8$ for both the trailing-edge designs with and without lands. Although the design without lands was found to have better overall cooling effectiveness compared with the design with lands, extensive investigations are still needed to balance the system integrity, structural strength and cooling effectiveness for the optimal design of turbine blades.

Acknowledgments

The authors want to thank Bill Rickard, Anand Gopa Kumar, and Hirofumi Igarashi of Iowa State University for their help in conducting the experiments, and Tom I. P. Shih of Purdue University for the helpful discussions on the experimental data analysis.

References

- [1] Taslim, M. E., Spring, S. D., and Mehlman, B. P., "An Experimental Investigation of Film Cooling Effectiveness for Slots of Various Exit Geometries," *Journal of Thermophysics and Heat Transfer*, Vol. 6, No. 2, 1992, pp. 302–307.
doi:10.2514/3.359
- [2] Uzol, O., Camci, C., and Glezer, B., "Aerodynamic Loss Characteristics of a Turbine Blade with Trailing Edge Coolant Ejection: Part 1- Effect of Cut-Back Length, Spanwise Rib Spacing, Free-Stream Reynolds Number, and Chordwise Rib Length on Discharge Coefficients," *Journal of Turbomachinery*, Vol. 123, No. 2, 2001, pp. 238–248.
doi:10.1115/1.1348017
- [3] Uzol, O., and Camci, C., "Aerodynamic Loss Characteristics of a Turbine Blade with Trailing Edge Coolant Ejection: Part 2- External Aerodynamics, Total Pressure Losses, and Predictions," *Journal of Turbomachinery*, Vol. 123, No. 2, 2001, pp. 249–257.
doi:10.1115/1.1351817
- [4] Martini, P., and Schulz, A., "Experimental and Numerical Investigation of Trailing Edge Film Cooling by Circular Wall Jets Ejected from a Slot with Internal Rib Arrays," *Journal of Turbomachinery*, Vol. 126, No. 2, 2004, pp. 229–236.
doi:10.1115/1.1645531
- [5] Martini, P., Schulz, A., and Bauer, H.-J., "Film Cooling Effectiveness and Heat Transfer on the Trailing Edge Cutback of Gas Turbine Airfoils With Various Internal Cooling Designs," *Journal of Turbomachinery*, Vol. 128, No. 1, 2006, pp. 196–205.
doi:10.1115/1.2103094
- [6] Holloway, S. D., Leylek, J. H., and Buck, F. A., "Pressure-Side Bleed Film Cooling: Part 1, Steady Framework for Experimental and Computational Results," ASME Paper GT-2002-30471, 2002.
- [7] Holloway, S. D., Leylek, J. H., and Buck, F. A., "Pressure-Side Bleed Film Cooling: Part 2, Unsteady Framework for Experimental and Computational Results," ASME Paper GT-2002-30472, 2002.
- [8] Medic, G., and Durbin, P. A., "Unsteady Effects on Trailing Edge Cooling," *Journal of Heat Transfer*, Vol. 127, No. 4, 2005, pp. 388–392.
doi:10.1115/1.1860565
- [9] Joo, J., and Durbin, P. A., "Simulation of Turbine Blade Trailing Edge Cooling," *Journal of Fluids Engineering*, Vol. 131, No. 2, 2009, pp. 021102-1–021102-14.
doi:10.1115/1.3054287
- [10] Ou, S., Han, J. C., Mehendale, A. B., and Lee, C. P., "Unsteady Wake over a Linear Turbine Blade Cascade with Air and CO₂ Film Injection. Part 1: Effect on Heat Transfer Coefficients," *Journal of Turbomachinery*, Vol. 116, No. 4, 1994, pp. 721–729.
doi:10.1115/1.2929465
- [11] Han, J. C., Dutta, S., and Ekkad, S., *Gas Turbine Heat Transfer and Cooling Technology*, Taylor and Francis, New York, 2000, pp. 540–559.
- [12] Saumweber, C., Schulz, A., and Witting, S., "Free-Stream Turbulence Effects on Film-Cooling with Shaped Holes," *Journal of Turbomachinery*, Vol. 125, No. 1, 2003, pp. 65–73.
doi:10.1115/1.1515336
- [13] Chyu, M. K., and Hsing, Y. C., "Use of a Thermographic Fluorescence Imaging System for Simultaneous Measurement of Film Cooling Effectiveness and Heat Transfer Coefficient," ASME Paper 96-GT-430, 1996.
- [14] Wright, L. M., Gao, Z., Varvel, T. A., and Han, J., "Assessment of Steady State PSP, TSP, and IR Measurement Techniques for Flat Plate Film Cooling," Summer Heat Transfer Conference, San Francisco, ASME Paper HT2005-72363, 2005.
- [15] Zhang, L., and Jaiswal, R. S., "Turbine Nozzle Endwall Film Cooling Study Using Pressure Sensitive Paint," *Journal of Turbomachinery*, Vol. 123, No. 4, 2001, pp. 730–738.
doi:10.1115/1.1400113
- [16] Ahn, J., Mhetras, S., and Han, J. C., "Film-Cooling Effectiveness on a Gas Turbine Blade Tip Using Pressure Sensitive Paint," ASME Paper GT2004-53249, 2004.
- [17] Choi, J. H., Mhetras, S., Han, J. C., Lau, S. C., and Rudolph, R., "Film Cooling and Heat Transfer on Two Cutback Trailing Edge Models with Internal Perforated Blockages," *Journal of Heat Transfer*, Vol. 130, No. 1, 2008, pp. 012201:1–012201:13.
doi:10.1115/1.2780174
- [18] Yang, Z., "Experimental Investigations on Complex Vortex Flows Using Advanced Flow Diagnostic Techniques," Ph.D. Dissertation, Aerospace Dept., Iowa State Univ., Ames, IA, 2009.
- [19] Kline, S. J., and McClintock, F. A., "Describing Uncertainties in a Single Sample Experiment," *Mechanical Engineering*, Vol. 75, No. 1, 1953, pp. 3–8.
- [20] Telisinghe, J. C., Ireland, P. T., Jones, T. V., Barrett, D., and Son, C., "Comparative Study Between a Cut-Back and Conventional Trailing Edge Film Cooling System," ASME Paper GT2006-91207, 2006.
- [21] Mukherjee, D. K., "Film Cooling with Injection Through Slots," *Journal of Engineering for Power*, Vol. 98, No. 4, 1976, pp. 556–559.
doi:10.1115/1.3446237
- [22] Chen, S. P., Li, P. W., Chyu, M. K., Cunha, F. J., and Abdel-Messeh, W., "Heat Transfer in an Airfoil Trailing Edge Configuration with Shaped Pedestals Mounted Internal Cooling Channel and Pressure Side Cutback," ASME Paper GT2006-91019, 2006.

J. Bons
Associate Editor